5-7-2013

Magnetic Properties of Fe Doped, Co Doped, and Fe+Co Co-Doped ZnO

J. J. Beltrán
Boise State University

J. A. Osorio
Universidad de Antioquia

C. A. Barrero
Universidad de Antioquia

Charles B. Hanna
Boise State University

A. Punnoose
Boise State University

Magnetic Properties of Fe Doped, Co doped and Fe+Co Co-Doped ZnO

J.J. Beltran
Grupo de Estado Sólido
Sede de Investigación Universitaria
Universidad de Antioquia, A.A. 1226
Medellín, Colombia.

Instituto de Química
Universidad de Antioquia, A.A. 1226
Medellín, Colombia

Department of Physics
Boise State University
Boise, Idaho 83725-1570, USA

J. A. Osorio
Grupo de Estado Sólido
Sede de Investigación Universitaria
Universidad de Antioquia, A.A. 1226
Medellín, Colombia.

C. A. Barrero
Grupo de Estado Sólido
Sede de Investigación Universitaria
Universidad de Antioquia, A.A. 1226
Medellín, Colombia.

C. B. Hanna
Department of Physics
Boise State University
Boise, Idaho 83725-1570, USA

A. Punnoose*
Department of Physics
Boise State University
Boise, Idaho 83725-1570, USA

*Correspondence author; e-mail: apunnoos@boisestate.edu, jjbj08@gmail.com

Abstract

The structural, electronic and magnetic properties of $Zn_{0.95}Co_{0.05}O$, $Zn_{0.95}Fe_{0.05}O$ and $Zn_{0.90}Fe_{0.05}Co_{0.05}O$ nanoparticles prepared by a sol-gel method are presented and discussed. X-ray diffraction and optical analysis indicated that high spin Co^{2+} ions substitute for the Zn^{2+} ions in tetrahedral sites. ^{57}Fe Mössbauer spectroscopy showed the presence of isolated paramagnetic Fe^{3+} ions in both Fe doped and Fe+Co co-doped ZnO, however, no evidence of ferromagnetically ordered Fe^{3+} ions is observed. In the $Zn_{0.95}Fe_{0.05}O$ sample, weak presence of $ZnFe_2O_4$ was detected as an impurity phase, whereas $Zn_{0.90}Fe_{0.05}Co_{0.05}O$ was impurity-free. Results of these studies suggest that Fe and Co ions in the Fe+Co co-doped sample has a strong synergistic effect because they eliminated the presence of impurities and gave the strongest ferromagnetic signal. Possible role of charge transfer ferromagnetism involving mixed valence ions is considered as a potential mechanism in these nanoparticles. Presence of both Co^{2+} and Fe^{3+} might promote more efficient charge transfer in the co-doped $Zn_{0.90}Fe_{0.05}Co_{0.05}O$, leading to the enhanced ferromagnetism observed in this sample. However, more evidence is necessary to confirm the role of charge transfer ferromagnetism.

I. INTRODUCTION

Transition metal (TM) doped ZnO has been proposed as one of the most promising candidates for dilute magnetic semiconductor (DMS) oxide materials with Curie temperature above room temperature (RT).[1] It is believed that the simultaneous presence of two kinds of dopants/defects,[2] especially multi-valence ions,[3] could tailor the position and occupancy of the Fermi energy of the materials and its magnetic behavior. Thus, co-doping ZnO simultaneously with Co^{2+} and Fe^{3+} might be a promising route to achieve and enhance RT ferromagnetism and such an investigation might help understand the origin of ferromagnetism (FM) and the mechanism of exchange interactions in TM doped metal oxides. Some previous works on ZnO prepared with co-doped TM showed the predicted increase in FM,[4-9, 12, 13, 14] while other studies have showed absence or reduction of FM.[9,10, 15] Thus, it is evident that the actual role and effect of co-doped TM ions in ZnO are not conclusive and in fact very conflicting. Therefore, more studies are required in order to improve our comprehension on the origin of the magnetism in these interesting compounds. For these reasons, individual samples of undoped, Fe doped, Co doped and Fe+Co co-doped ZnO at the same concentration of 5% were prepared and their structural, optical and magnetic properties were investigated.

II. EXPERIMENTAL

Nanocrystalline powders of $Zn_{1-x}M_xO$ (x= 0 and 0.05) with M=Fe or Co and $Zn_{1-2x}Fe_xCo_xO$ (x= 0.05) nanoparticles with sizes in the range of 19–47 nm were prepared by the polymeric precursor method based on the modified Pechini process, described in detail elsewhere.[16] Required amounts of $Zn(NO_3)_2{\cdot}6H_2O$, $Co(NO_3)_2{\cdot}6H_2O$, $Fe(NO_3)_3{\cdot}9H_2O$ and citric acid were used for preparing the samples. The nanopowder samples were characterized by x-ray diffraction (XRD) using a Phillips X'Pert X-ray diffractometer with a Cu-Kα source (λ= 1.5406Å). The XRD patterns were fitted using the Rietveld method to obtain structural parameters. The optical absorption spectra were measured in the range of 200–800 nm using a UV–VIS–NIR scanning spectrometer (Shimadzu, Japan). ^{57}Fe Mössbauer spectra were recorded at RT using a conventional Mössbauer spectrometer working at constant acceleration and the spectra were fitted with Lorentzian line shape. Magnetic properties of the nanopowders were studied using a Quantum Design, model 6000 PPMS system.

III. RESULTS AND DISCUSSION

Fig. **1** displays the XRD refined patterns of undoped, Fe doped, Co doped and Fe+Co co-doped ZnO nanopowders. The XRD patterns showed only the wurzite phase of ZnO with no evidence of any secondary phases suggesting that the doped TM ions are incorporated into the host ZnO lattice. For undoped ZnO, an average crystallite size (*Dv*) of 37nm was estimated using the Scherrer formula.[17] Interestingly, a *Dv* = 47nm was obtained for 5% Co doped ZnO indicating significant grain growth, while 5% Fe doping caused an opposite effect with *Dv* = 19nm. The *Dv* of the Co+Fe co-doped ZnO sample was 25nm, indicative of their combined effect. Both cell parameters *a* and *c* of ZnO, calculated from the refinement, showed significant decrease with doping, with Fe doping causing more lattice contraction compared to Co doping. The lattice volume *V* decreased from 47.8Å^3 in ZnO to 47.7Å^3 for 5% Co doped ZnO and to 47.5Å^3 in both 5% Fe doped sample as well as the Co+Fe co-doped sample. Assuming tetrahedral environment and high spin state, the ionic radii of Co^{2+}(0.58 Å) and Fe^{3+}(0.49 Å) ions are smaller than Zn^{2+} (0.60 Å) [18] and this can explain the observed changes in *a*, *c* and *V* in these samples and acts as strong proof of dopant incorporation into the ZnO structure. It is worth mentioning that the introduction of Co as a co-dopant into Fe doped ZnO sample slightly improves the crystallinity of wurzite; as observed by Dienesha *et al*. also.[14]The average Zn–O bond length (*L*) in ZnO (1.987Å) parallel to the *c*-axis[19,20] gave a minimum for the Fe doped sample (1.983Å) and is higher in Co doped (1.984Å) and Fe+Co co-doped ZnO (1.986Å) samples. Also, in a stoichiometric wurtzite structure the *c/a* ratio is 1.633.[20] Our pure as well as doped samples showed significantly smaller *c/a* ratio (1.602±0.001) and this might indicate the presence of oxygen vacancies and extended defects.[20]

Fig. 2 shows the absorption spectra of the different nanopowders and the band gap (*Eg*) obtained following the Kubelka–Munk rule.[21, 22] Both the Co doped and Co+Fe co-doped samples clearly display the well known d-d transitions around 567, 610 and 655 nm, characteristic of high spin tetrahedral Co^{2+} ions [23, 24] substituted at the Zn^{2+} ions in the ZnO structure. The lower *Eg* (= 3.29 eV) of undoped ZnO compared to that of the bulk (3.3 eV)[25] might be associated with the presence of oxygen vacancies.[26] Compared to the undoped ZnO sample, all the doped samples show a decrease in *Eg* (see Fig. 2b), with Co doped ZnO displaying the lowest *Eg* (= 2.90 eV) and the Co+Fe co-doped sample at *Eg* = 3.12 eV. Such decrease in *Eg* due to TM doping has been attributed to the *sp-d* spin-exchange interactions between the band electrons and the localized d electrons of the transition-metal ion substituting the cation.[27] In the absence of a strong correlation between *Eg* and *Dv*, the observed decrease of *Eg* with TM doping could be a consequence mainly of Co and/or Fe incorporation (substitutional and/or interstitial) into the ZnO wurzite structure along with charge-compensating oxygen vacancies and introduction of other possible defects.

Fig 3 shows the ^{57}Fe Mössbauer spectra of Fe doped and Fe+Co co-doped ZnO nanopowders at RT and the hyperfine parameters obtained by fitting. In both samples, presence of ferromagnetic impurities such as metallic iron, FeCo clusters, iron oxides or $CoFe_2O_4$ or their superparamagnetic particles are clearly ruled out based on the Mössbauer parameters. [28, 29] To analyze the Mössbauer spectra of both $Zn_{0.95}Fe_{0.05}O$ and $Zn_{0.90}Fe_{0.05}Co_{0.05}O$, a model including two doublets corresponding to two paramagnetic Fe^{3+} ions occupying highly distorted tetrahedral sites[30] located at different chemical environments of ZnO (see Fig. 3) was used . In Fe doped ZnO the necessity of a third doublet is evident due to presence of a small shoulder located at the central part of the spectrum. The hyperfine parameters (δ=0.34 mm/s, Δ=0.37 mm/s and A= 13 %) of this additional doublet 3 matches well with that of $ZnFe_2O_4$. This must be a very weak impurity phase in $Zn_{0.95}Fe_{0.05}O$ to escape complete detection by XRD.[31] In contrast, the spectrum of Fe+Co co-doped $Zn_{0.90}Fe_{0.05}Co_{0.05}O$ sample is more symmetric and does not show this doublet 3, suggesting that Co^{2+} might be preventing the formation of $ZnFe_2O_4$ in the Fe+Co co-doped sample. The hyperfine parameters of doublet 1 (D1) is assigned to Fe^{3+} ions in less distorted and/or less defective sites, whereas doublet 2 (D2) comes from Fe^{3+} ions close to more defective sites or close to oxygen vacancies.[16, 32] Note that the fit-derived values of Δ and Γ for D2 in Fe doped ZnO are higher than those of the same doublet in Fe+Co co-doped sample. This points to higher concentrations of oxygen vacancies/defects and a wider distribution of Fe^{3+} distorted sites in the Fe doped ZnO, and that Co^{2+} ions in the Co+Fe co-doped ZnO might be reducing the concentration and distribution of oxygen vacancies/defects. The complete absence of a sextet in $Zn_{0.95}Fe_{0.05}O$ and $Zn_{0.90}Fe_{0.05}Co_{0.05}O$ samples suggests that at RT the doped Fe^{3+} ions are not magnetically interacting and they have no contribution to the observed ferromagnetism in these samples.

Fig. 4 shows the RT *M–H* curves of $Zn_{0.95}Co_{0.05}O$, $Zn_{0.95}Fe_{0.05}O$ and $Zn_{0.90}Fe_{0.05}Co_{0.05}O$ samples, where the linear paramagnetic component has been subtracted to illustrate the actual M_s and H_c (lower inset Fig. 4) of the FM phase. The Fe doped and Co doped ZnO samples showed a weak FM behavior, with open hysteresis loops (upper inset of Fig. 4). However, the Fe+Co co-doped sample showed a much stronger ferromagnetism characterized by a ~9-fold increase in the saturation magnetization and moderate increase in coercivity compared to the ZnO samples doped with only Fe or Co.

What could be the origin of the observed FM in Co doped and Fe doped ZnO samples and more importantly the 9-fold increase in FM when ZnO is co-doped with both Fe and Co? Optical and Mössbauer spectroscopic data confirm the presence of high spin Co^{2+} and Fe^{3+} ions respectively, in our samples. Absence of sextet spectra in the Mössbauer data suggest that there is no ferromagnetic coupling between the doped Fe^{3+} ions and the presence of doublets confirm that the doped Fe^{3+} ions are in isolated paramagnetic state. Thus, the moments of the Fe^{3+} ions are not contributing to the observed ferromagnetism, at least in the Fe containing $Zn_{0.95}Fe_{0.05}O$ and $Zn_{0.90}Fe_{0.05}Co_{0.05}O$ samples. It is noteworthy that *Eg* decreased in all the doped samples suggesting that changes in the magnetic behavior may be related to changes in the electronic structure of ZnO due to the incorporation of the dopants and the resulting oxygen vacancies/defects. Recently Coey *et al.*[4] proposed a new model for ferromagnetism based on charge transfer in metal oxides in which the dopants exist in mixed valence states. Here, the role of the doped TM ions is to provide electrons locally into the conduction band or to accept electrons from it. Electrons resulting from change in the valence state of the TM ions can be transferred to local defect states that exist at the nanoparticle surface and/or other regions. If the energy gain from Stoner splitting of the local density of states exceeds the energy required for transferring electrons, the surface states could develop a magnetic moment via spontaneous Stoner ferromagnetism and order the surface region (or other defect-rich regions) of the particle ferromagnetically while the core of the particle remain paramagnetic. Thus, the magnetic moment of the doped TM ions and exchange coupling between them do not play any role in the ferromagnetism, and what matters is their ability to exhibit mixed valence.

Presence of both Co^{2+} and Fe^{3+} ions in the Co+Fe co-doped sample provides a powerful charge reservoir to facilitate stronger ferromagnetism in this sample. More studies to investigate possible charge transfer between these 3d ions and the presence of other valence states of Co and Fe are necessary to fully confirm the role of charge transfer ferromagnetism in these samples and this will be investigated in future. Other mechanisms could also be considered as possible sources of this enhanced magnetic signal of the co-doped sample such as the carrier-mediated ferromagnetism. Additional experiments to quantify the amount of carriers and defects introduced will be required to fully unravel the actual mechanism.

IV. CONCLUSIONS

The simultaneous presence of Fe and Co greatly improves the ferromagnetic signal of ZnO nanoparticles in comparison to the presence of only one of these cations. Simultaneous doping of these two ions increased the coercivity and saturation magnetization, and also eliminated the formation of the $ZnFe_2O_4$ impurity phases. The presence of Fe^{3+} ions in the co-doped samples in the isolated paramagnetic state with no indication of any magnetic coupling between them suggests that the ferromagnetism in this material may not be related to the magnetic moment of the dopant ions. Possible role of charge transfer ferromagnetism involving mixed valence ions and the increment of the carrier density concentration might be considered as potential mechanisms, although more evidence is necessary to confirm this.

ACKNOWLEDGMENTS

The authors are grateful to CODI (sustainability program for Solid State Group 2011-2012 and to Gobernación del Cesar by technical cooperation agreement No 0.38 2006 Colciencias-Universidad Popular del Cesar in association with the Universidad de Antioquia. The work at Boise State University was supported in part by NSF EAGER DMR-1137419, ARO W911NF-09-1-0051, NSF CBET 1134468 and NSF DMR-0906618 grants.

REFERENCES

[1]T. Dietl, H. Ohno, F. Matsukura, J. Cibert, D. Ferrand, Science **287**,1019 (2000)
[2] N. N. Lathiotakis, A. N. Andriotis, M. Menon, Phys. Rev. B **78**, 193311 (2008)
[3] J M D Coey, KwanruthaiWongsaprom1, J Alaria, M Venkatesan, J. Phys. D: Appl. Phys. **41** 134012 (2008)
[4] H. Li, Y. Huang, Q. Zhang, Y. Qiao, Y. Gu, J. Liu, Y. Zhang, Nanoescale **3**, 654 (2011)
[5] R.Viswanatha, D. Naveh, J.R. Chelikowsky, L. Kronik, D. D. Sarma J. Phys. Chem. Lett. 3, 2009 (2012)
[6] R. N.Aljawfi, S.Mollah, J.Magn.Magn.Mater **323**, 3126 (2011)
[7] Y. Q. Wang, L. Su, L. Liu, Z. M. Tian, T. Q. Chang, Z. Wang, S. Y. Yin, S. L. Yuan, Phys. Status Solidi A **207**, No. 11, 2553 (2010)
[8] D. Y. Inamdar, A. D. Lad, A.K. Pathak, I. Dubenko, N. Ali,S. Mahamuni, J. Phys. Chem. C **114**, 1451 (2010)
[9] W. Yan, Z. Sun, Q. Liu, T.o Yao, Q. Jiang, F. Hu,Y. Li, J. He, Y.Peng, S, Wei, Appl. Phys. Lett. **97**, 042504 (2010).
[10] C. N. R. Rao, F. L. Deepak, J. Mater. Chem. **15**, 573 (2005)
[11] H. Liu, J.i Yang, Z. Hua, Y. Liu, L. Yang, Y. Zhang, J. Cao, Mater. Chem. Phys. **125**, 656 (2011)
[12] Y. M. Cho, W. K. Choo, H. Kim, D. Kim, and Y. E. Ihm, Appl. Phys. Lett. **80**, 3358 (2002)
[13] L. Q. Liu, B. Xiang, X. Z. Zhang, Y. Zhang, and D. P. Yu, Appl. Phys. Lett. **88**, 063104 (2006)
[14] M.L. Dinesha, H.S. Jayanna, S. Mohanty, S. Ravi, J. Alloys Compd. **490**, 618 (2010)
[15] D. Karmakar, T. V. C. Rao, J. V. Yakhmi, A. Yaresko, V. N. Antonov, R. M. Kadam, S. K. Mandal, R. Adhikari, A. K. Das, T. K. Nath, N. Ganguli, I. Dasgupta, G. P. Das, Phys. Rev. B **81**, 184421 (2010)
[16] J. J. Beltran , L. C. Sánchez ,J. Osorio, L. Tirado, E. M. Baggio-Saitovitch, C. A. Barrero, J Mater Sci **45**, 5002 (2010)
[17] B.D. Cuttity, Elements of X-ray Diffraction, Second ed., Addision-Wesley Publishing Company, Inc., Reading, MA, USA, 1978, p. 555
[18] R.D. Shannon, Acta Cryst. A. **32**, 751 (1976)
[19] S. Ilican ,Y. Caglar, M. Caglar, J. Optoelectron Adv. Mater. **10**, No. 10 2578 (2006)
[20] Hadis Morkoç, Ümit Özgü. "*Zinc Oxide. Fundamentals, Materials and Device Technology*" 2009 WILEY-VCH Verlag GmbH & Co. KGaA, Weinheim
[21] P. Kubelka, F. Munk, Tech. Phys. **12**, 593 (1931)
[22] P. Kubelka, J. Opt. Soc. Am. **38**, 448 (1948)
[23] S. Ramachandran, A.Tiwari, J. Narayan Appl. Phys. Lett. **84**, 5255 (2004)
[24] Z. Jin, T. Fukumura, M. Kawasaki, K. Ando, H. Saito, Appl. Phys. Lett. **78**, 3824 (2001).
[25] A. Shalimov, W. Paszkowicz, K. Grasza, P. Skupiński, A. Mycielski, J. Bak-Misiuk, Phys. Stat. Sol. (b) 244, No. 5, 1573 (2007)
[26] Wang Y G, Lau S P, Lee H W, Yu S F, Tay B K, Zhang X H and Hng H H 2003 *J. Appl. Phys.* **94** 354
[27] X. Xu, C. Cao J. Alloys Compd. **501**, 265 (2010)
[28] S. Ayyappan, J. Philip, B. Raj , J. Phys. Chem. C **113**, 590 (2009)
[29] P. Chandramohan, M.P. Srinivasan, S.Velmurugan,S .V.Narasimhan J. Solid State Chem. **184**, 89 (2011)
[30] E. Murad, and J. Cashion "*in Mössbauer spectroscopy of environmental materials and their industrial utilization"*, Kluwer Academic Publishers, Boston, 2004
[31] S.J. Stewart, S.J.A. Figueroa M.B. Sturla, R.B. Scorzelli, F. Garcia, F.G. Requejo, Physica B **389** 155–158 (2007)
[32] K. Nomura, C. A. Barrero, J. Sakuma, M. Takeda, Phys. Rev. B **75**, 184411 (2007)

FIGURE CAPTIONS

FIG. 1. (Color online) Rietveld refinement analysis of XRD patterns of undoped, Co doped, Fe doped and Fe+Co co-doped ZnO nanopowders. Solid spheres are experimental data, whereas red solid lines represent the fit. The blue lines below represent the difference pattern.

FIG. 2 (Color online) (a) Optical absorbance spectra of ZnO, $Zn_{0.95}Co_{0.05}O$, $Zn_{0.95}Fe_{0.05}O$ and $Zn_{0.90}Fe_{0.05}Co_{0.05}O$ samples. (b) Variation of the calculated band gap with the dopant type. The dashed line represents *Eg* of bulk ZnO.

FIG. 3 (Color online) RT ^{57}Fe Mössbauer spectra of $Zn_{0.95}Fe_{0.05}O$ and $Zn_{0.90}Fe_{0.05}Co_{0.05}O$ samples along with theoretical simulations. Mössbauer parameters for D1 and D2 obtained by fitting the spectra are also shown. Isomer shifts (δ), quadrupole splittings (Δ) and linewidths (Γ) are given in mm/s and relative areas (A) in %. Mössbauer parameters for D3 are presented in the text.

FIG. 4. (Color online) RT hysteresis loops from Fe doped, Co doped and Fe+Co co-doped ZnO samples. Upper inset shows the low field region for Fe doped and Co doped ZnO samples, while lower inset shows the variations in coercivity H_c and saturation magnetization M_s with the dopant type.

FIGURES

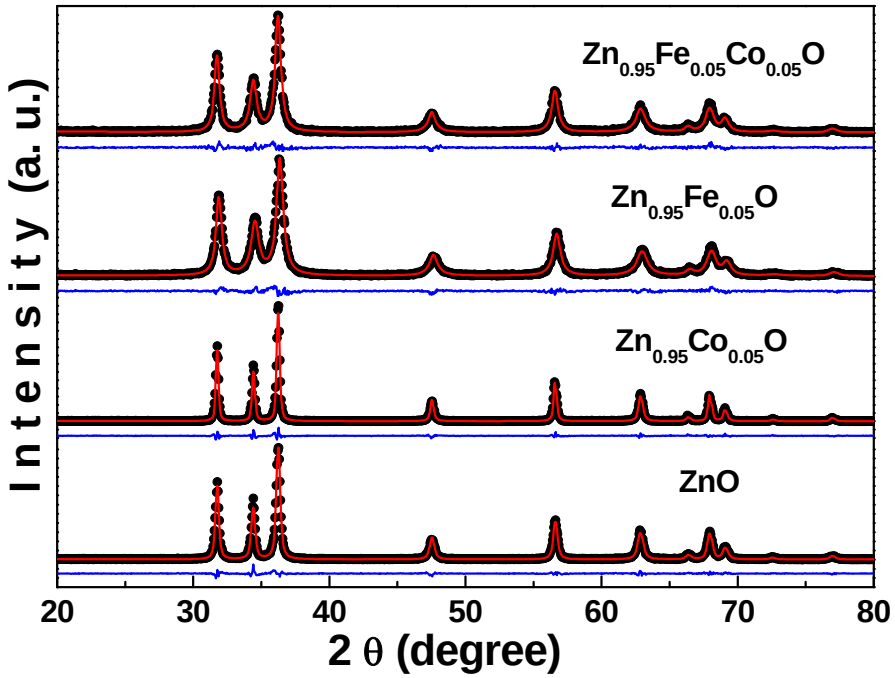

FIG. 1. (Color online)

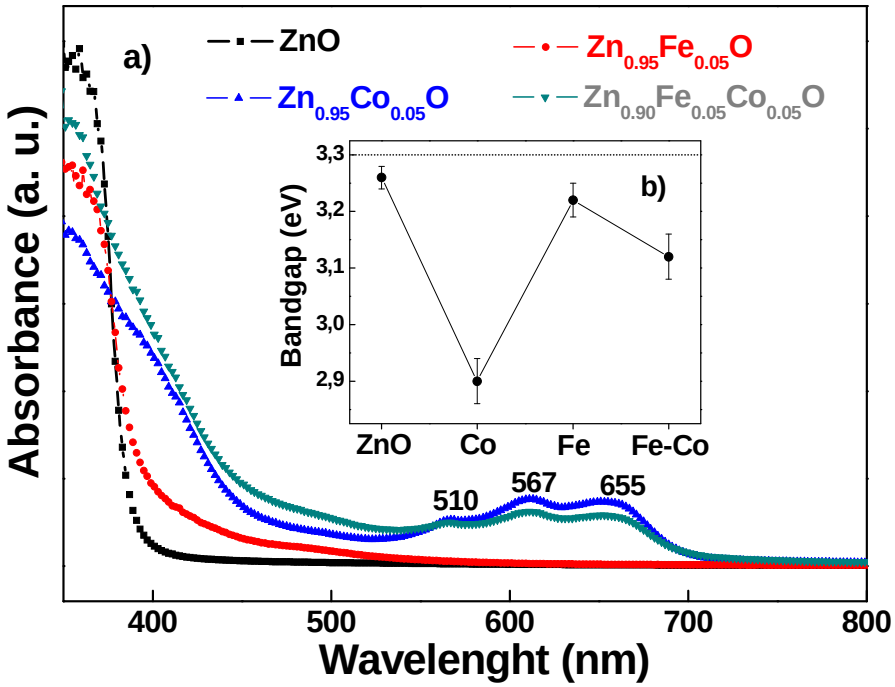

FIG. 2. (Color online)

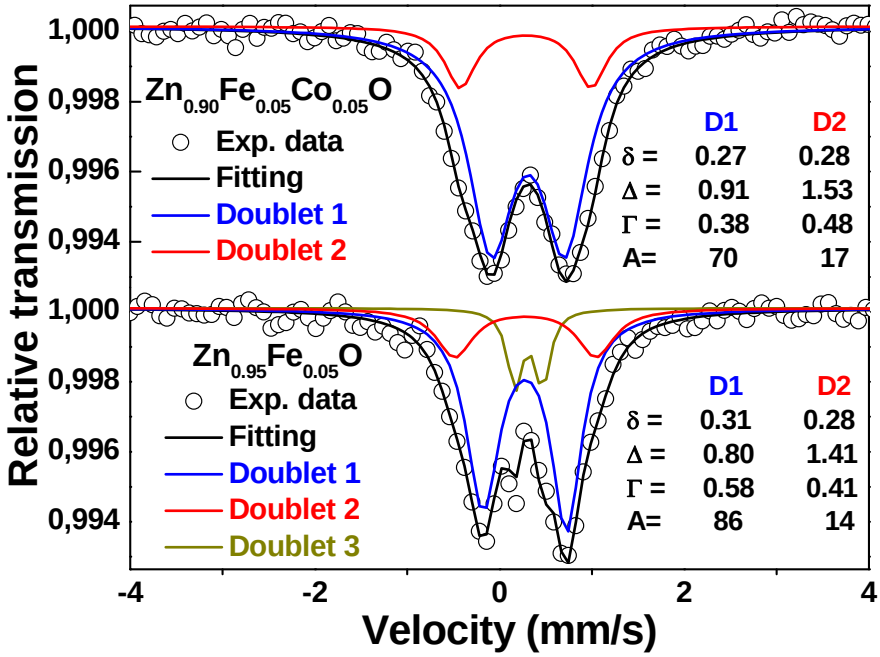

FIG. 3. (Color online)

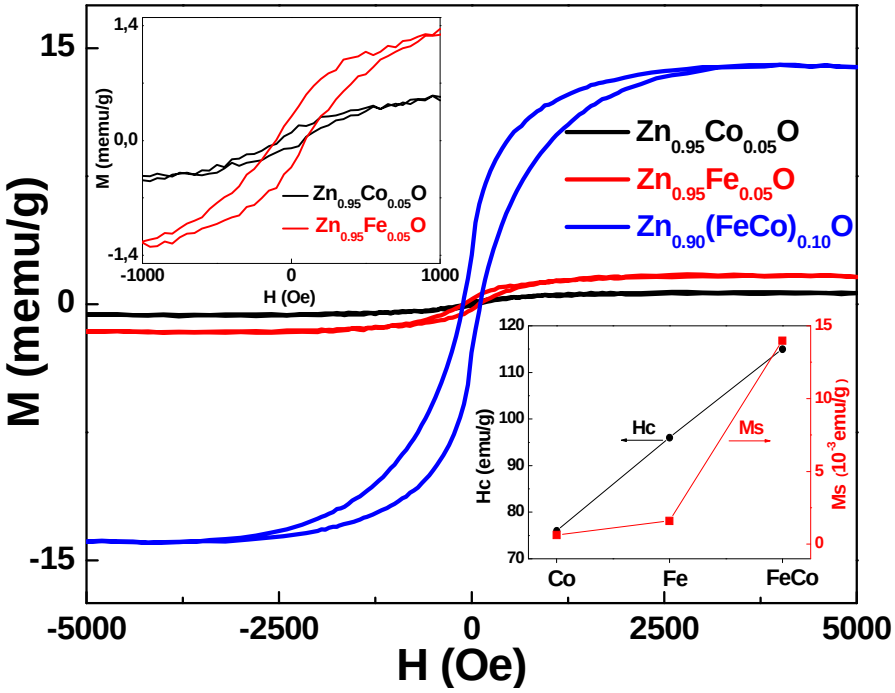

FIG. 4. (Color online)